Plasma Performance Improvement by Advanced High Field Side Pellet Injection in ASDEX Upgrade

A. Lorenz, P.T. Lang, J.C. Fuchs, J. Gafert, O. Gehre, O. Gruber, G. Haas, M. Kaufmann, B. Kurzan, M. Maraschek, V. Mertens, H.W. Müller, H.D. Murmann, J. Neuhauser, W. Schneider, ASDEX Upgrade Team

Max-Planck-Institut für Plasmaphysik, EURATOM Association, Boltzmannstr. 2, 85748 Garching, Germany

e-mail: axel.lorenz@ipp.mpg.de

Abstract. Limited available pellet velocities so far restricted the plasma performance of the efficient launch scheme from the tokamak magnetic high field side. Although pellet injection during H-mode results in more peaked density profiles and enhanced performance with respect to gas puff refuelling, prompt particle and energy losses induced by pellet induced ELM bursts still limited the operational area. An improved pellet injection set-up applied at ASDEX Upgrade allowed for the first time significantly higher injection velocities. In first proof-of-principle plasma discharges a successful scan of pellet injection at v = 240 - 1200 m/s and plasma parameter studies at v = 560 m/s were completed. They resulted in deeper penetration and particle deposition mitigating fast particle and energy losses. Further extension of tokamak operation in the high density regime seems feasible.

1. Introduction

Injection of pellets produced from frozen hydrogen isotopes is currently the most developed advanced method to refuel a toroidally confined fusion plasma [1]. This has been established in a series of studies although conventional pellet injection from the magnetic low field side (LFS) showed particularly in strongly auxiliary heated plasmas poor fueling efficiency similar to that of gas puffing. In contrast, pellet injection from the high field side (HFS) first performed on ASDEX Upgrade was found to yield significant extensions of the tokamak operation space by refueling steady state H-mode discharges near the empirical Greenwald density limit with only little loss of energy confinement [2]. The reason is a fast radial drift of the high-β-plasmoid forming around the ablating pellet and rapidly transferring part of the pellet mass in major radius direction [3,4].

However, in currently operating tokamaks access to the HFS is complicated by virtually irremovable pellet accelerators installed for LFS injection close to the torus outboard and has to be gained via strongly curved guide tubes. During tube transfer with repeated wall impacts the fragile nature of cryogenic D_2 imposes a speed limit of a few hundred m/s on the pellets leading to still shallow deposition profiles where pellet induced ELM bursts cause rapid onset of enhanced edge barrier transport. The temporal barrier breakdown gives rise to a strong convective energy loss, finally limiting the operational boundary achievable under steady state pellet refuelling [5]. Modelling the impact of different pellet induced particle deposition profiles under typical H-mode conditions showed that deeper deposition would delay and mitigate the ELM induced losses. Therefore, judging by the velocity dependence of the LFS injection [6], larger pellet velocities seem an option to improve mass deposition from the HFS provided the pellet penetration in the 100-1000 m/s velocity range is not completely governed by the dynamics of the curvature drift alone.

At ASDEX Upgrade a systematic pellet impact study [7] has lead to the design of a new pellet guiding system to transfer pellet at speeds close to 1000 m/s. The scheme used in the present study is a preliminary, faster to build version used in order to get results before a 9 months shutdown of ASDEX Upgrade. After a concise description of the new pellet transfer scheme results of first plasma discharges are presented in this paper.

2. Apparatus and Experimental Set-up

2.1 The new loop design

The new pellet guiding system, displayed in Fig. 1, employs a looping geometry. The major design constraint was the location of the ASDEX Upgrade pellet accelerator, which is a centrifuge [8]. The issue was solved by a 180°-rotation of the accelerator such that pellets were ejected away from the tokamak and then guided back to the torus HFS by a roughly elliptical track. The geometry settled most problems of previous guiding schemes. Pellets do not undergo large angle collisions (a < 2°) and they are forced into a controlled trajectory making use of reduced friction between pellet and track surface due to formation of a vapor film [9] without putting excessive centrifugal pressure on the pellets. The loop consists of three elliptic parts: a) a funnel to collect the scattered pellets from the centrifuge, b) a guiding tube element including a diagnostic section and c) a guiding track segment in the torus port to link up with the plasma. Use of this port set the poloidal injection angle to about 70° with respect to the horizontal axis.

The funnel has not only to compensate for the horizontal scatter of the centrifuge but also to guide the pellets into the elliptic curvature. As described in detail in ref. 7 the horizontal scatter led to the design of convex funnel walls diverting in the first part to follow the scatter (for up to 100 mm) and focussing into a 6 mm wide exit. In order to simplify the realisation of the following (guide tube) segment, the funnel length was tailored to fill a quarter of an ellipse (L = 4.76 m). The guide tube segment is a proof-of-principle version installed by glueing a 7 mm ID teflon tube concentrically into an elliptically fixed 13 mm ID copper tube. The 9 m long segment is followed by a 1 m diagnostic section situated as close as possible to the plasma. The diagnostics incorporate a double light barrier and shadowgraphy complex. The last segment, tokamak port, puts extreme stress on the pellet with curvature radii changing between 25 m and 1.4 m because of the specific port geometry (2 m long, 50 mm ID) and the poloidal injection angle. Two free flight zone have to be crossed by the pellets due to vacuum valves. Alignment here is performed by means of "guiding track negatives" fitting exactly into the 5x5 mm u-type track groove on either side of the valve.

All segments of the guiding system were separately tested before commissioning the entire scheme. The funnel was studied in-situ where incoming pellets hit the side walls at about 0.2 m after the funnel entrance. Only about 1% of pellets at all speeds were registered broken at this point which is a vast improvement on the previous funnel destroying most pellets at v > 560 m/s. The guide tube and torus port segments were tested in the laboratory using a gas gun [10] and 3 mm cylindrical pellets. Whereas the torus port section was the version to be installed at ASDEX Upgrade, the guide tube section was simulated by a 8 - 12 m long spirale-type circles with 1m long sections of curvature radii decreasing from R = 5 to 1 m. Critical survival speeds of 850 - 900 m/s were found for the torus port section. whereas guide tube schemes were tested for two tube versions, a 13 mm ID copper tube and a 7 mm ID teflon tube with the first allowing for pellet speeds of 750 -800 m/s, the latter for 800 - 850 m/s which obviously led to its choice as preliminary guide tube section.

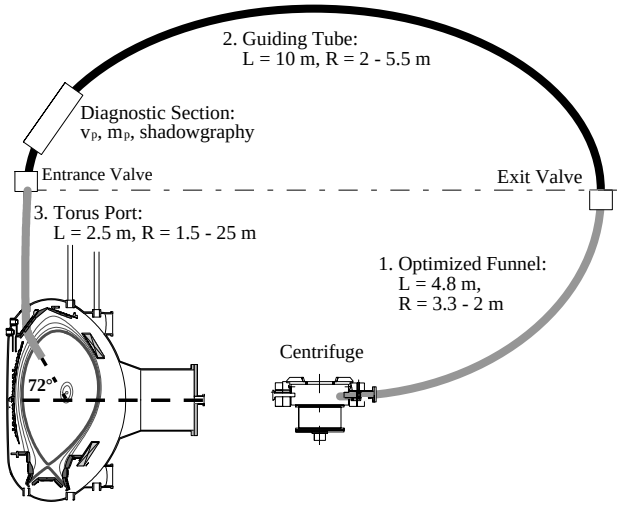

FIG. 1. Schematic view of the preliminary pellet injection system at ASDEX Upgrade for high speed launch from the torus inside (not to scale).

2.2. Target plasma and injection scenarios

Injection into plasma discharges was performed using pre-programmed pellet sequences of about 2 s duration at moderate repetition rates of 10 - 30 Hz. Plasmas with I_p = 1 MA, B_t = 2.7 T, q_{95} = 3.8, low triangularity were driven by approx. 6 MW H_0 NB injection into a stationary ELMy H-mode phase, the base density before (and after) the pellet sequence was adjusted to approx. $3.5 \cdot 10^{19}$ m^3 by hydrogen gas puffing. The cryopump with 100 m^3/s pumping speed was applied together with turbomolecular pumps (14 m^3/s) for efficient particle exhaust. The DCN laser interferometer system was equipped with special input electronics to avoid perturbations by the pellet induced density increase. Six YAG lasers were fired in bursts to yield a record of the time evolution of density and temperature profiles at 2 ms resolution. The repetition rate of the burst sequence was slightly detuned from the pellet repetition rate to sample all phases of the post pellet density decay. This way, several pellet deposition profiles were recorded in each shot as density profiles before and almost immediately after pellet injection were measured.

3. Pellet Injections into Plasma Discharges

3.1. Pellet survival in the loop

In order to avoid mechanical resonances operation of the centrifuge was limited to four frequencies corresponding to v = 240, 560, 880, 1200 m/s. Operational tests of the assembled guiding system included shadowgraphy and speed loss measurements in the diagnostic section, i.e. after 15 m track length. Almost 100% of the pellets survived the transfer at v = 240 and 560 m/s, which has not been achieved before. At v = 880 m/s still 1/3 of the pellets survived, at v = 1200 m/s all pellets were destroyed at this point. Fig. 2 depicts 2 mm D_2-pellet cubes pressed to the track ($R \approx 2$ m). Although pellets at v = 248 m/s and 562 m/s look identical, statistically only half of the pellets are as large at v = 560 m/s. The other half are intact pellets showing stronger erosion. At 880 m/s this ratio is halfed again accompanied by a larger erosion (sometimes exceeding 50%) for most of the intact pellets. In contrast, examining two pieces of a broken pellet, the erosion seems weaker (see Fig. 2d). Speed loss measurements showed a minor, almost constant loss of about 5 m/s across v = 240 - 1200 m/s. Thus pellets lost only 2% at v = 240 m/s down to 0.4% at v = 1200 m/s. In conclusion, at v = 880 m/s an expected critical speed level of the currently installed guiding track was reached, therefore first stage refueling studies concentrated on v = 240 and 560 m/s.

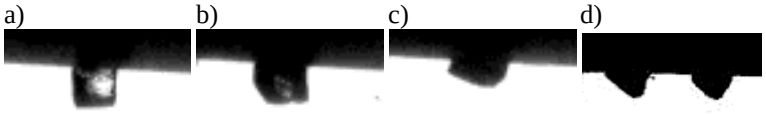

FIG. 2. Shadowgraphs from 2 mm ice cubes at L = 15 m: a) v = 248 m/s, b) v = 562 m/s, c) and d) v = 882 m/s.

3.2. Pellet penetration and mass deposition

Figs. 3 and 4 summarize early observations of penetration depths and particle deposition profiles for both pellet velocities. The pellet penetration depths mapped onto the horizontal axis are taken by using the temporal evolution of the total visible ablation radiation assuming constant velocity along the injection path. At v = 240 m/s, a penetration depth Δ, of 16.5±1.5 cm was determined, whereas Δ = 21.2±1.0 cm was found for v = 560 m/s. A wide angle video camera watching the pellet path displayed a larger margin of 8 - 10 cm deeper penetration by the faster pellets as shown in Fig. 4. This was recorded despite some 20% mass loss of the faster pellets estimated from the particle inventory enhancement calculated from the density

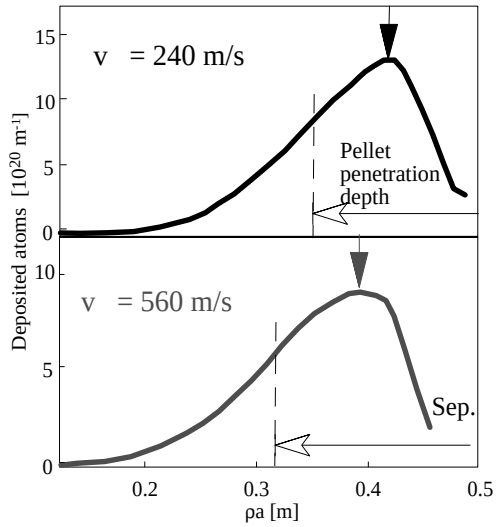

FIG. 3. Typical particle deposition profiles derived from DCN laser interferometer and Li beam data (solid line) before and after pellet injection. Pellet penetration mapped onto the horizontal axis (arrows) is given as well.

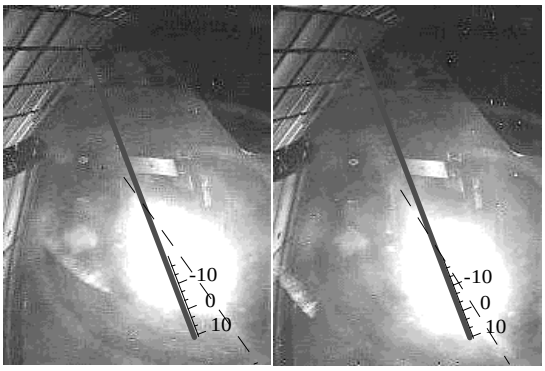

FIG. 4. Wide angle video frames of pellet ablation clouds, left: v = 240 m/s, right: v = 560 m/s, spatial dimension arbitrary [cm]

profile deconvolution from the DCN laser interferometer signals and the Li beam edge profiles. The relative improvement of Δ with increasing pellet speed is in surprisingly good agreement with the empirical IPADBASE [6] scaling derived for LFS pellets yielding $\Delta \sim m_P^{5/27} \cdot v_P^{1/3}$ and predicting a ratio of $\Delta_{560}/\Delta_{240} = 1.27$, which is quite close to the experimental value of 1.28. However, the absolute penetration depths are strongly enhanced for the HFS injection with respect to this scaling giving 9 and 12 cm for 240 and 560 m/s, respectively. Notably, possible outward pellet acceleration by the radial drift of the ablatant was not taken into account. However, in most video frames the slower pellet ablation clouds describe a larger poloidal angle (dashed line) with respect to v = 560 m/s as seen in Fig. 4 by the deviation from the designated injection path (full line).

The higher velocity causes not only deeper pellet penetration but also a clear shift of particle deposition (see Fig. 3) towards the hotter centre with respect to the ablation region. This effect is enhanced by the acceleration of the high-β plasmoid supposed to be scaling with temperature [4], and a more pronounced signature is expected in hotter next step fusion plasmas. A shift of particle deposition towards the core is clearly visible with respect to the ablation region. This fast particle drift has been observed in many HFS launch experiments [4,11,12] and is attributed to the radial curvature drift acting on the pellet ablatant [3,4].

3.3. ELM zone traversal

The ELM induced, prompt particle and energy losses indicated by the rapid density decay during the first phase after pellet injection were mitigated at v = 560 m/s. The faster pellet is still followed by a phase of enhanced ELM activity, causing the particle losses and W_{MHD} reduction, however, the magnitude is significantly reduced with respect to the slower pellet. Statistical analysis using pellets of about the same mass launched at about the same target density but with different velocities yielded an averaged n_e-decay time for the ELM burst phase of 49.0±2.2 ms for the slow and 58.2±1.3 ms for the fast pellets. The power lost transiently in the first phase after each injected pellet was determined as 1.05±0.18 MW for the slow and 0.84±0.14 MW for the fast pellets. After termination of the pellet induced ELMs, W_{MHD} starts to recover its initial unperturbed value. Notably, the faster pellets showed a somewhat higher probability of triggering sawteeth. The occurrence of a sawtooth in the post-pellet phase again slightly increased particle and energy losses. This behaviour was attributed to the deeper penetration and particle deposition of the faster pellets. However, most pellets did not trigger sawtooth and carefully chosen q-profiles might avoid this problem in future discharges [13].

4. Conclusions

A new optimized pellet guiding system has been commissioned for HFS plasma fuelling in ASDEX Upgrade. In proof-of-principle experiments first evidence was found that higher pellet launch velocity from the HFS leads to deposition of particles deeper inside the plasma. Correlated to this is the alleviation of pellet induced ELMs and a reduction of the particle and energy loss rate in the phase shortly after pellet injection (10-20 ms in ASDEX Upgrade). Although the curvature drift of the pellet induced ablation plasmoid seems to cause the deeper penetration, it does not dominate the pellet ablation completely. Since similar speed dependences of the penetration depths for LFS and HFS injection seem to hold, the curvature drift obviously modifies the pellet ablation shielding factor. Reduced in LFS injection by stripping off the pellet plasma shield in hot plasmas [3], the shielding is enhanced in the HFS scheme due to precooling of the plasma at the forefront of the pellet. Further optimisation of the guiding track should enable to build an HFS-database to scale to ITER-like fusion plasmas to define more closely demands of pellet injection systems for large scale fusion plasmas.

[1] ITER Phsics Basis Editors et al., Nucl. Fusion, **39** (1999) 2137.
[2] P.T. Lang et al., Nucl. Fusion, **40** (2000) 245.
[3] M. Kaufmann, K. Lackner, L. Lengyel, and W. Schneider, Nucl. Fusion, **26** (1986) 171.
[4] H.W. Müller et al., Phys. Rev. Lett., **83** (1999) 2199.
[5] P.T. Lang et al., to be published in Controlled Fusion and Plasma Physics (Proc. 27th Eur. Conf. Budapest, 2000, P3.045)
[6] L.R. Baylor et al., Nucl. Fusion, **37** (1997) 445.
[7] A. Lorenz, P.T. Lang, R.S. Lang, Rev. Scient. Instr., **71** (2000) 3736.
[8] C. Andelfinger et al., Rev. Scient. Instr., **64** (1993) 983.
[9] B.S. Gottfried, C.J. Lee, K.J. Bell, Int. J. Heat Mass Transfer **9**, (1966) 1167
[10] W. Riedmüller, Report IPP 4/188, Max-Planck-Institut f. Plasmaphysik, (1980).
[11] J. deKloe et al., Phys. Rev. Lett. **82** (1999) 2685.
[12] L.R. Baylor et al., Phys. Plas. **7** (2000) 1878.
[13] S. Günter et al., Nucl. Fusion **38** (1998) 1431.